

Science

 AAAS

**Direct Targeting of Light Signals to a Promoter
Element-Bound Transcription Factor**

Jaime F. Martínez-García, *et al.*

Science **288**, 859 (2000);

DOI: 10.1126/science.288.5467.859

***The following resources related to this article are available online at
www.sciencemag.org (this information is current as of February 3, 2009):***

Updated information and services, including high-resolution figures, can be found in the online version of this article at:

<http://www.sciencemag.org/cgi/content/full/288/5467/859>

This article **cites 41 articles**, 17 of which can be accessed for free:

<http://www.sciencemag.org/cgi/content/full/288/5467/859#otherarticles>

This article has been **cited by** 247 article(s) on the ISI Web of Science.

This article has been **cited by** 98 articles hosted by HighWire Press; see:

<http://www.sciencemag.org/cgi/content/full/288/5467/859#otherarticles>

This article appears in the following **subject collections**:

Botany

<http://www.sciencemag.org/cgi/collection/botany>

Information about obtaining **reprints** of this article or about obtaining **permission to reproduce this article** in whole or in part can be found at:

<http://www.sciencemag.org/about/permissions.dtl>

REPORTS

A remarkable up-down asymmetry in the nystagmus, together with the strong vestibular input to up-BT cells, appears to suggest an additional vestibular imbalance. The region where we injected muscimol contained up-BT neurons and no down eye movement cells. Because up-BT neurons received excitatory inputs from the anterior semicircular canals, their inactivation might be expected to result in downward drift of the eye due to a decreased anterior canal input. Instead, the eye drifted upward in a wide oculomotor range, suggesting increased, rather than decreased, signals from the anterior canal.

What is the neural mechanism that produces the central vestibular imbalance of anterior canal dominance? Up-BT neurons probably project to the flocculus, which has a unique connection pattern with the vertical canal system. Only anterior canal-related vestibular nucleus neurons receive floccular inhibition (12). Therefore, inactivation of the up-BT neurons may reduce the activity of Purkinje cells, leading to disinhibition of vestibular neurons that receive inputs from the anterior canal. These vestibular neurons then exhibit increased discharge. The anterior canal input to the brainstem circuitry is increased while the posterior canal input remains unchanged. This idea is supported by a similar downbeat nystagmus after floccular lesions (1). This experiment thus suggests that the PMT-flocculus-vestibular nucleus pathway is important in maintaining vestibular balance. It should be noted, however, that the asymmetry of nystagmus we observed does not necessarily indicate an imbalance of vestibular inputs to the neural integrator. The PMT-flocculus pathway may be involved in an intrinsic mechanism of the integrator that sets the neutral eye position.

It is known that the cerebellum is necessary for normal operation of the brainstem neural integrators (1, 3, 4). The cerebellum must acquire oculomotor signals from the brainstem. This study suggests that our up-BT neurons relay eye position information to the flocculus. Furthermore, the effect of inactivation of up-BT cells indicates their importance in the oculomotor integration. The caudal pontine PMT area may be a new component of the neural integration system for vertical, and perhaps horizontal, eye movement, along with the midbrain interstitial nucleus of Cajal, vestibular nuclei, and nucleus prepositus hypoglossi.

References and Notes

1. D. S. Zee, A. Yamazaki, P. H. Butler, G. Gücer, *J. Neurophysiol.* **46**, 878 (1981).
2. D. A. Robinson, in *Basic Mechanisms of Ocular Motility and Their Clinical Implications*, G. Lennerstrand and P. Bach-y-Rita, Eds. (Oxford Univ. Press, New York, 1975), pp. 337–374.
3. D. A. Robinson, *Brain Res.* **71**, 195 (1974).
4. B. Y. Kamath and E. L. Keller, *Math. Biosci.* **30**, 341 (1976); D. S. Zee, R. J. Leigh, F. Mathieu-Millaire, *Ann. Neurol.* **7**, 37 (1980).
5. J. A. Büttner-Ennever, A. K. E. Horn, K. Schmidtke, *Rev. Neurol.* **145**, 533 (1989); J. A. Büttner-Ennever and A. K. E. Horn, *Ann. N.Y. Acad. Sci.* **781**, 532 (1996).
6. S. Nakao, I. Curthoys, C. H. Markham, *Brain Res.* **183**,

291 (1980); G. Cheron, S. Saussez, N. Gerrits, *J. Neurophysiol.* **74**, 1367 (1995).

7. Five adult cats were prepared for recording of neuronal activity in the brainstem. All experiments were done with the permission of the Animal Experiment Committee of the University of Tsukuba, which is operated in accordance with Japanese Governmental Law (no. 105). A coil was implanted subconjunctivally under pentobarbital sodium anesthesia and aseptic conditions to measure eye movement by a magnetic-search coil technique (13). The tympanic bulla on each side was opened, and silver-ball electrodes were implanted on the round window to stimulate the vestibular nerve. After recovery from surgery, each animal was trained to accept restraining conditions without stress. A position 16.5° nose up from the stereotaxic horizontal was taken as a zero vertical position. This was near the center of the vertical oculomotor range. Glass-coated tungsten electrodes were used for extracellular recordings. Care was taken to ensure that the recording was from a cell body and not from an axon. Only negative-positive spikes with a duration (time to positive peak) of >250 μ s were regarded as action potentials of the soma. These unit spikes could be recorded not only during advancement but also during withdrawal of the electrode, another indication of somatic recording. The MLF was identified physiologically by recording monosynaptic volleys from the vestibular nerves and by monosynaptic activation of secondary vestibular axons, which all exhibited initial positivity. The explored region extended rostrocaudally from 2.0 mm anterior to 1.5 mm posterior of the rostral pole of the abducens nucleus and ventrally to 3.5 mm from the floor of the fourth ventricle. The lateral limit of the region extended from the midline to about 1.5 mm. The tonic firing rate of a cell was defined as an average rate for the fixation period. The size of the burst component for a given saccade was estimated by subtracting the eye position-dependent component from the total number of spikes [see (14)]. For natural vestibular stimulation, the turntable was rotated sinusoidally in the light in
8. W. Graf and K. Ezure, *Exp. Brain Res.* **63**, 35 (1986); R. A. McCrea, A. Strassman, S. M. Highstein, *J. Comp. Neurol.* **264**, 571 (1987).
9. S. C. Cannon and D. A. Robinson, *J. Neurophysiol.* **57**, 1383 (1987).
10. E. Godaux, P. Mettens, G. Cheron, *J. Physiol. London* **472**, 459 (1993); P. Mettens, E. Godaux, G. Cheron, H. L. Galiana, *J. Neurophysiol.* **72**, 785 (1994).
11. J. D. Crawford, W. Cadera, T. Vilis, *Science* **252**, 1551 (1991).
12. Y. Sato and T. Kawasaki, *J. Neurophysiol.* **64**, 551 (1990).
13. A. F. Fuchs and D. A. Robinson, *J. Appl. Physiol.* **21**, 1068 (1966).
14. S. Chimoto, Y. Iwamoto, K. Yoshida, *J. Neurophysiol.* **81**, 1199 (1999).
15. Supported by Core Research for Evolutionary Science and Technology of Japan Science and Technology Corporation. We thank S. Shoji for helpful comments.

22 November 1999; accepted 3 March 2000

Direct Targeting of Light Signals to a Promoter Element-Bound Transcription Factor

Jaime F. Martinez-Garcia, Enamul Huq, Peter H. Quail*

Light signals perceived by the phytochrome family of sensory photoreceptors are transduced to photoresponsive genes by an unknown mechanism. Here, we show that the basic helix-loop-helix transcription factor PIF3 binds specifically to a G-box DNA-sequence motif present in various light-regulated gene promoters, and that phytochrome B binds reversibly to G-box-bound PIF3 specifically upon light-triggered conversion of the photoreceptor to its biologically active conformer. We suggest that the phytochromes may function as integral light-switchable components of transcriptional regulator complexes, permitting continuous and immediate sensing of changes in this environmental signal directly at target gene promoters.

Plants use a set of sensory photoreceptors to monitor the environment for informational light signals (1). The phytochrome (phy) family, comprising five members (phyA to phyE) in

Department of Plant and Microbial Biology, University of California, Berkeley, CA 94720, and U.S. Department of Agriculture–Agricultural Research Service Plant Gene Expression Center, 800 Buchanan Street, Albany, CA 94710, USA.

*To whom correspondence should be addressed. E-mail: quail@nature.berkeley.edu

Arabidopsis, track the red (R) and far red (FR) light wavelengths by virtue of their capacity for photoinduced, reversible switching between two conformers: the R-absorbing, biologically inactive Pr form and the FR-absorbing, biologically active Pfr form. Each phy molecule is a dimer of subunits that consist of a \approx 125-kD polypeptide with a covalently bound tetrapyrrole chromophore that is autocatalytically attached by the apoprotein (2). Light-driven Pfr formation induces changes in the expression of numerous genes underlying various aspects of

REPORTS

tion was rapidly reversed by reconversion to Pr. These data indicate that phyB recognition of DNA-bound PIF3 requires maintenance of the photoreceptor in the biologically active (Pfr) form.

The G-box motif is neither present in all light-regulated promoters, nor is it confined to light-regulated genes. On the contrary, it is found in a broad range of plant gene promoters responsive to a diversity of nonlight-related stimuli (3, 22–26, 29, 30). Moreover, most studies aimed at identifying plant DNA-binding proteins that recognize this motif report the cloning of bZIP class factors rather than bHLH proteins (22, 30). To address this apparent complexity in relation to PIF3, we examined whether PIF3 was capable of recognizing the G-boxes in photoresponsive genes in the context of their native flanking sequences. This is pertinent because the nucleotides flanking the core hexamer E-box motif have been shown to influence the specificity of bHLH family-member recognition of binding sites containing this core motif (31, 32). Figure 3B shows that the G-box-containing sequences from the promoters of four light-regulated genes, *RBCS-1A*, *CCA1*, *LHY*, and *SPA1*, all interacted effectively with PIF3, despite deviations from the consensus sequence of the PIF3 binding site (Fig. 1A) at the positions flanking the CACGTG hexanucleotide core in some cases (Fig. 3A). To determine whether PIF3 might recognize non-G-box motifs in other functionally defined LREs in photoresponsive genes, we examined PIF3 binding to the GT1, Z, and GATA motifs representing consensus sequences from several light-regulated promoters (33). PIF3 exhibited no detectable interaction with these motifs (Fig. 3C), further verifying the sequence-specific nature of the G-box recognition. Together the data indicate that PIF3 is indeed capable of sequence-specific binding to the G-box-containing promoters of a variety of light-regulated genes.

To determine whether PIF3 is necessary for the phytochrome-regulated expression of these genes, we examined the effect of continuous R light (Rc) on their mRNA levels in wild-type and PIF3-antisense (17) seedlings. The rapid (within 1 hour) Rc-induced increase in expression of *CCA1* and *LHY* was reduced in the PIF3-antisense seedlings (Fig. 4, A and B). By contrast, the similarly rapid increase in *SPA1* expression was unaffected in the antisense plants. Two more slowly induced genes also showed no difference in expression between wild-type and antisense plants. These were the G-box-containing gene *RBCS-1A* (34) and *CHS* (Fig. 4, A and B) for which there is no evidence of a functionally active, fully palindromic G-box in *Arabidopsis* (22, 35, 36). On the other hand, the absence of the HY5 bZIP protein in the *hy5* null mutant (37) caused no reduction in the photoresponsiveness of *CCA1*, *LHY*, or *SPA1*, but markedly reduced the induc-

tion of *CHS* (Fig. 4, C and D). Together these data suggest that there are multiple classes of promoters in phytochrome-responsive genes: G-box-containing promoters that require PIF3 for responsiveness; G-box-containing promoters that do not require PIF3 for responsiveness, despite their capacity to bind PIF3 in vitro; and promoters lacking evidence of functionally active G-boxes that do not require PIF3 for responsiveness, but nevertheless do require the bZIP factor HY5, considered to be a G-box-binding protein, for responsiveness.

On the basis of this pattern of expression profiles, we suggest that a subclass of rapidly induced genes, represented by *CCA1* and *LHY*, may be direct targets of phytochrome regulation through binding of the photoreceptor to PIF3, which is in turn bound to G-box promoter elements. Other subclasses of phytochrome-responsive genes apparently have alternative response pathways independent of PIF3. It is intriguing that *CCA1* and *LHY* encode similar

MYB-class proteins that have been implicated in phytochrome-regulated *CAB* gene expression and/or circadian clock regulation (38–40). It is possible, therefore, that PIF3 represents the entry point for phytochrome regulation of the plant circadian clock, as well as initiating one branch of the phytochrome-induced gene expression cascade (41).

The data presented here and elsewhere (17, 20, 21, 28) suggest that the phytochromes may integrate into, and function as photoswitchable components of, transcription-regulator complexes directly at target promoter sites after light-induced translocation from cytoplasm to nucleus (Fig. 5). The function of PIF3 in this scheme would be to recruit phyB specifically to the designated promoters. Regardless of the biochemical basis of the ensuing signaling transactions between phyB and the transcriptional machinery, the data suggest that plants have evolved a mechanism whereby an extracellular signal can be monitored continuously

Fig. 2. PIF3 simultaneously binds G-box DNA and the active form of phyB (PfrB). (A) Design of experiments in (B). PHYB refers to full-length phytochrome B apoprotein. phyB refers to photoactive phytochrome B, after chromophore attachment to PHYB, depicted by the small black rectangle (42). After incubation of proteins with labeled G-wt probe, the samples were given a pulse of FR or R (46) and incubated on ice in the dark (Dk) for 2 additional hours before EMSA. (B) The binding complex formed between PIF3 and the G-wt probe is shifted in the presence of R-irradiated photoactive phyB, and this supershifted complex is dependent on full-length PIF3. Lane 1, no protein; lane 2, mock-translated TnT; lanes 3, 7, and 11, 2 μ l of PHYB; lanes 4, 5, 8, 9, 12, and 13, 2 μ l of phyB; lanes 6 to 9, PIF3; lanes 10 to 13, G:hbPIF3. (C) Experimental design for (D). Either phyB alone (lanes 3 and 4) or PIF3 and phyB together (lanes 5 to 12) were incubated for 3 hours in the dark (Dk) after being given a R and/or FR pulse, before G-box probe addition and EMSA. After an initial R pulse (R) (lanes 3 and 5 to 8) a FR pulse was given either immediately [R + FR(0)], after 1 hour [R + FR(1)], or 2 hours [R + FR(2)] (lanes 6, 7, and 8, respectively). Conversely, after an initial FR pulse (FR) (lanes 4 and 9 to 12), a R pulse was given immediately [FR + R(0)], after 1 hour [FR + R(1)], or 2 hours [FR + R(2)] (lanes 10, 11, and 12, respectively). (D) The R-induced shift in the PIF3-G-wt probe binding complex caused by the presence of phyB is photoreversible. Lane 1, mock-translated TnT; lanes 2 and 5 to 12, PIF3; lanes 3 to 12, 2 μ l of phyB. Proteins responsible for the binding complexes are indicated to the right. FP, free probe; (*) nonspecific binding complex; PfrB, biologically active form of phyB, formed by R pulse.

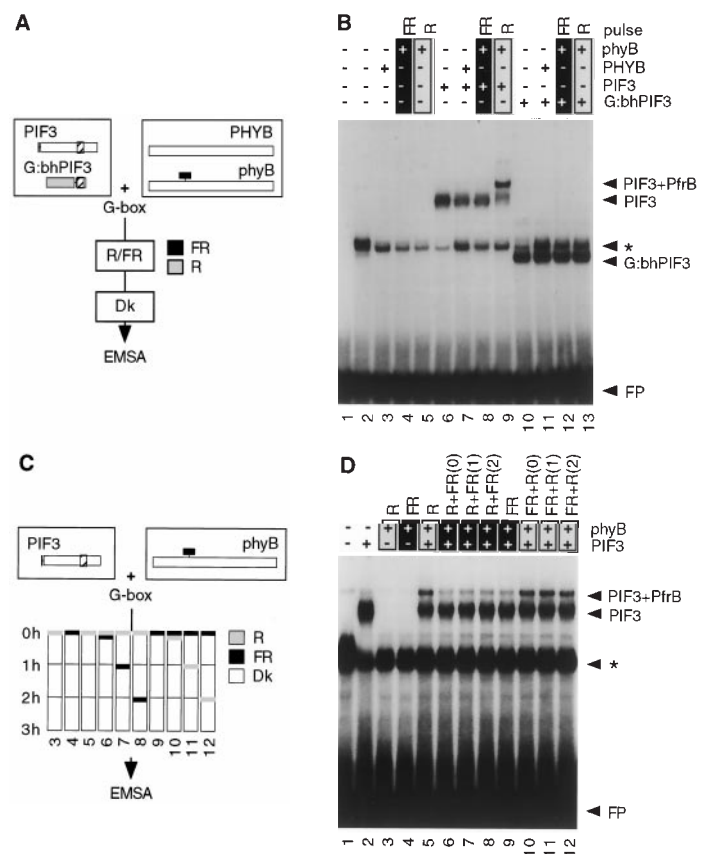


Fig. 3. PIF3 binds to G-box-containing promoter sequences from various light-regulated genes. (A) Upper-strand nucleotide sequences of the probes used in the EMSA experiments in (B) and (C). The probes contain G-box and surrounding sequences from *RBCS-1A* (25), *CCA1* (38, 39), *LHY* (40), and *SPA1* (14) promoters. The G-box sequence is highlighted in bold and the coordinates are in parentheses. (B) Competition of PIF3 binding to G-wt by the different G-box sequences from the four light-regulated genes. Lanes 1 and 6, mock-translated TnT; lanes 2 to 5, 7 to 16, PIF3; lanes 3, 8, 11, and 14, 5× molar excess of cold probe; lanes 4, 9, 12, and 15, 25× molar excess of cold probe; lanes 5, 10, 13, and 16, 125× molar excess of cold probe; lanes 3 to 5, *RBCS-1A*/G-box cold probe; lanes 8 to 10, *CCA1*/G-box cold probe; lanes 11 to 13, *LHY*/G-box cold probe; lanes 14 to 16, *SPA1*/G-box cold probe. (C) PIF3 binding to labeled G-wt probe is competed only by the LRE that contains a G-box (47). Lanes 1 to 9, PIF3; lanes 2, 4, 6, and 8, 25× molar excess of cold probe; lanes 3, 5, 7 and 9, 125× molar excess of cold probe; lanes 2 and 3, GT1 cold probe; lanes 4 and 5, Z cold probe; lanes 6 and 7, G cold probe; lanes 8 and 9, GATA cold probe (47).

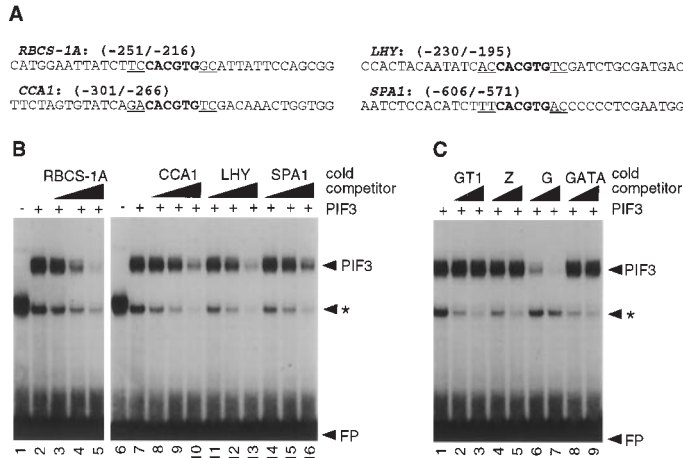
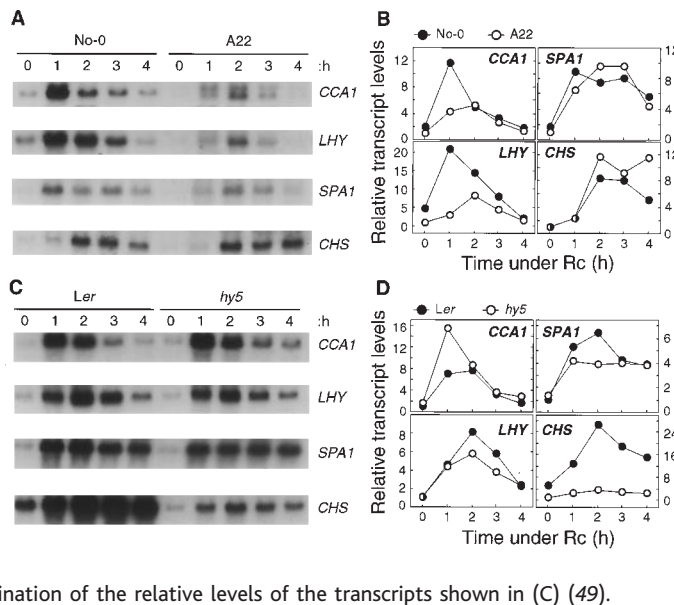


Fig. 4. The light-induced expression of *CCA1* and *LHY* is reduced in the PIF3 *Arabidopsis* antisense line A22. (A) RNA blot analysis of *CCA1*, *LHY*, *SPA1*, and *CHS* mRNA levels in the A22 line (17) and its corresponding wild type (No-0) in Rc for increasing periods (48). (B) Quantitative determination of the relative levels of the transcripts shown in (A) (49). (C) RNA blot analysis of *CCA1*, *LHY*, *SPA1*, and *CHS* mRNA levels in a *hy5* mutant line [*hy5-1* allele (37)] and its corresponding wild-type (*Ler*) (48). (D) Quantitative determination of the relative levels of the transcripts shown in (C) (49).



and directly by the control elements of target genes, thereby potentially permitting almost instantaneous modulation of transcription rates in response to changes in signal content.

References and Notes

1. R. E. Kendrick and G. H. M. Kronenberg, *Photomorphogenesis in Plants* (Kluwer, Dordrecht, Netherlands, ed. 2, 1994).
2. P. H. Quail, *Plant Cell Environ.* **20**, 657 (1997).
3. W. B. Terzaghi and A. R. Cashmore, *Annu. Rev. Plant Physiol. Plant Mol. Biol.* **46**, 445 (1995).
4. G. C. Whitelam and P. F. Devlin, *Plant Cell Environ.* **20**, 752 (1997).
5. P. H. Quail, *Philos. Trans. R. Soc. London* **353**, 1399 (1998).
6. G. C. Whitelam, S. Patel, P. F. Devlin, *Philos. Trans. R. Soc. London Ser. B* **353**, 1445 (1998).
7. X.-W. Deng and P. H. Quail, *Semin. Cell Dev. Biol.* **10**, 121 (1999).
8. M. Ahmad, and A. R. Cashmore, *Plant J.* **10**, 1103 (1996).

9. G. C. Whitelam *et al.*, *Plant Cell* **5**, 757 (1993).
10. D. Wagner, U. Hoecker, P. H. Quail, *Plant Cell* **9**, 731 (1997).
11. U. Hoecker, Y. Xu, P. H. Quail, *Plant Cell* **10**, 19 (1998).
12. M. S. Soh, S. H. Hong, H. Hanzawa, M. Furuya, H. G. Nam, *Plant J.* **16**, 411 (1998).
13. M. Hudson, C. Ringli, M. T. Boylan, P. H. Quail, *Genes Dev.* **13**, 2017 (1999).
14. U. Hoecker, J. M. Tepperman, P. H. Quail, *Science* **284**, 496 (1999).
15. C. Fankhauser *et al.*, *Science* **284**, 1539 (1999).
16. G. Choi *et al.*, *Nature* **401**, 610 (1999).
17. M. Ni, J. M. Tepperman, P. H. Quail, *Cell* **95**, 657 (1998).
18. W. R. Atchley and W. M. Fitch, *Proc. Natl. Acad. Sci. U.S.A.* **94**, 5172 (1997).
19. T. Littlewood and G. I. Evan, *Helix-Loop-Helix Transcription Factors* (Oxford Univ. Press, New York, 1998).
20. R. Yamaguchi, M. Nakamura, N. Mochizuki, S. A. Kay, A. Nagatani, *J. Cell Biol.* **145**, 437 (1999).
21. S. Kircher *et al.*, *Plant Cell* **11**, 1445 (1999).
22. E. Menkens, U. Schindler, A. R. Cashmore, *Trends Biochem. Sci.* **20**, 506 (1995).

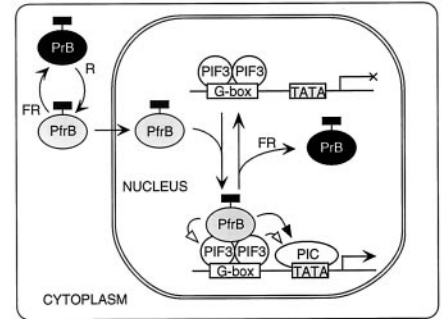


Fig. 5. Model depicting the proposed mechanism of phyB regulation of gene expression. R-induced conversion of phyB from its cytoplasmically localized, biologically inactive Pr form (PrB) to its active Pfr form (PfrB) triggers translocation to the nucleus (20, 21), where it binds to PIF3 that is constitutively nuclear (17) and bound as a presumptive dimer to G-box motifs in target promoters. Bound PfrB then activates (or represses) transcription either directly, by functioning as a coregulator in recruiting and/or biochemically or allosterically modifying components of the preinitiation complex (PIC) or associated factors (solid arrowhead), or indirectly, by biochemically or allosterically modifying the presumptive transcriptional regulatory activity of PIF3, which then in turn recruits coregulator or PIC components (open arrowheads). Subsequent reconversion by FR of bound PfrB to PrB causes rapid dissociation of the photoreceptor from DNA-bound PIF3, disrupting the enhanced (or reduced) transcriptional activity of target genes. In the short term, subsequent reconversion by R of PrB to PfrB, either before dissociation or nearby in the nucleoplasm, would rapidly reestablish the previous enhanced (or reduced) transcriptional state.

23. G. Argñello-Astorga and L. Herrera-Estrella, *Annu. Rev. Plant Physiol. Plant Mol. Biol.* **49**, 525 (1998).
24. F. Ishige, M. Takaichi, R. Foster, N.-H. Chua, K. Oeda, *Plant J.* **18**, 443 (1999).
25. R. G. K. Donald and A. R. Cashmore, *EMBO J.* **9**, 1717 (1990).
26. S. Chattopadhyay, L.-H. Ang, P. Puente, X.-W. Deng, N. Wei, *Plant Cell* **10**, 673 (1998).
27. G. Patikoglou and S. K. Burley, *Annu. Rev. Biophys. Biomol. Struct.* **26**, 289 (1997).
28. M. Ni, J. M. Tepperman, P. H. Quail, *Nature* **400**, 781 (1999).
29. M. E. Williams, R. Foster, N.-H. Chua, *Plant Cell* **4**, 485 (1992).
30. X. Niu, L. Renshaw-Gegg, L. Miller, M. J. Guiltinan, *Plant Mol. Biol.* **41**, 1 (1999).
31. F. Fisher and C. R. Goding, *EMBO J.* **11**, 4103 (1992).
32. T. Shimizu *et al.*, *EMBO J.* **16**, 4689 (1997).
33. P. Puente, N. Wei, X.-W. Deng, *EMBO J.* **15**, 3732 (1996).
34. J. F. Martínez-García and P. H. Quail, unpublished data.
35. E. Schäfer, T. Kunkel, H. Frohnmeyer, *Plant Cell Environ.* **20**, 722 (1997).
36. L.-H. Ang *et al.*, *Mol. Cell* **1**, 213 (1998).
37. T. Oyama, Y. Shimura, K. Okada, *Genes Dev.* **11**, 2983 (1997).
38. Z.-Y. Wang *et al.*, *Plant Cell* **9**, 491 (1997).
39. Z.-Y. Wang and E. M. Tobin, *Cell* **93**, 1207 (1998).
40. R. Schaffer *et al.*, *Cell* **93**, 1219 (1998).
41. D. E. Somers, P. F. Devlin, S. A. Kay, *Science* **282**, 1488 (1998).
42. Binding reactions were performed with GST:PIF3:Flag, His6:PIF3, G:hbPIF3, and phyB. The PIF3 coding sequence was amplified by polymerase chain reaction (PCR). The Flag peptide sequence was added to the 3' reverse primer, and the PCR product was cloned into Eco RI-Not I-digested pGEX-4T-1 vector, to give pGFP. GST:PIF3:flag protein was produced in *Escherichia coli*

(BL21 cells) transformed with pGPF, and the fusion protein was purified by using sequentially both Glutathione Sepharose 4B (Pharmacia Biotech) and anti-Flag M2 affinity gel (Eastman Kodak) beads. This protein was used only for RBSS experiments (Fig. 1A). His₆-PIF3, G:hhPIF3, and phyB proteins were produced by transcription and translation (TnT) systems (Promega). PIF3 coding sequence was amplified by PCR and cloned into pRSETb vector (Invitrogen). The resulting fusion protein contains a His₆-tag at the NH₂-terminal end and was used throughout the work (referred to as PIF3 in the figures). G:hhPIF3 corresponds to GST (glutathione S-transferase) (Fig. 1D, gray box) fused to the PIF3 bHLH domain (from residue 340 to 397; cross-hatched box). The PIF3 bHLH domain was amplified by PCR and cloned in pGEX-4T-1. The resulting coding region was amplified with oligonucleotides that added the T7 promoter sequence upstream of the first ATG, and the PCR product was directly used as a template in the TnT reaction. The full-length *Arabidopsis* PHYB apoprotein was produced by TnT reaction, and the chromophore was autocatalytically attached (28).

43. The binding reactions were performed essentially as described [J. F. Martínez-García and P. H. Quail, *Plant J.* **18**, 173 (1999)] with modifications. The binding buffer was supplemented with 10% glycerol and 0.05% NP-40, and nonspecific competitor used was 50 ng of poly(dI-dC). poly(dI-dC) per reaction. The binding complexes were resolved by EMSAs in 4% polyacrylamide gel in 0.5× tris-borate EDTA buffer at room temperature (90 min at 10 V cm⁻¹), and the gels were dried and autoradiographed.
44. F. R. Cantón and P. H. Quail, *Plant Physiol.* **121**, 1207 (1999).
45. RBSS was performed as described [T. K. Blackwell and H. Weintraub, *Science* **250**, 1104 (1990)] with modifications. We synthesized 60-base oligonucleotides of which the middle 12 bases consist of random sequences (5'-GTCTGTCTGGATCCGAGGTGAGTA-N12-ACGTCTCCGAAGCTTACGTCGCC-3'). Two 20-base oligonucleotides were also synthesized as forward (5'-GTCTGTCTGGATCCGAGGTG-3') and reverse (5'-CGC-GACGTAAGCTTCGGAAG-3') primers. The stringency of RBSS was increased by increasing the amount of nonspecific competitor (50, 100, 200, 400, and 500 ng, from first to fifth cycles, respectively) and by decreasing the amount of protein [2, 2, 1, 1, and 1 μl of TnT-expressed PIF3 (42), or 500, 500, 500, 250, and 250 ng of *E. coli*-purified GST:PIF3:flag protein (42), from first to fifth cycle, respectively] and the amount of labeled DNA probe [90,000 cpm (~10⁶ cpm μg⁻¹) for the first round; 20,000 cpm of high-specific activity probe from second to fifth cycle] in the binding reaction (43). After five rounds of selection, the retarded DNA was amplified by PCR, digested with Bam HI-Hind III, and cloned into pBluescript. Individual clones were randomly selected and sequenced. The sequences were aligned centered around the identified G-box motif.
46. Light sources are described in (28). Pulses were 2 min of FR (88 μmol m⁻² s⁻¹) or R light (88 μmol m⁻² s⁻¹).
47. The selected LREs used [GT1, 4× (5'-TGTTGGTTA-ATATG-3'); Z, 2× (5'-ATCTATTCGTATACGTCGAC-3'); G, 4× (5'-TGACACGTCGCA-3'); and GATA, 4× (5'-AAGATAAGATT-3')] have been described elsewhere (33).
48. After germination, seedlings were grown in the dark at 22°C for 4 days. Material was harvested at various times after 0, 1, 2, 3, and 4 hours of exposure to continuous red light (R; 20 μmol m⁻² s⁻¹). Total RNA was isolated with the RNeasy Plant Miniprep kit (Qiagen). For RNA analyses, 5 μg of total RNA were loaded per lane, and then transferred to MSI Nylon membranes. The membranes were hybridized in Church buffer at 65°C overnight with random primer-labeled fragments (CCA1, *LHY*, *CHS*, *SPA1*). CCA1 and *LHY* probes were amplified by PCR from *Arabidopsis* DNA with the use of specific primers, cloned, and confirmed by sequencing. The CCA1 probe (amplified with the primers 5'-GCAGCTGCTAGTGCTTGGTGGGCT-3' and 5'-TCA-TGTGGAAGCTTGAGTTTCCAA-3') corresponded to positions 2082 to 3010 in the 3' region of the main open reading frame (ORF) (38, 39); the *LHY* probe (amplified with the primers 5'-CATGCTGCAGCTACATTCGGT-GCT-3' and 5'-TCATGTAGAAAGCTTCTCTTCCAATCG-3') corresponded to positions 1271 to 2275 in the 3'

region of the main ORF (40). Southern blot analysis showed no detectable cross-hybridization between CCA1 and *LHY* probes under the washing conditions used (34). The *SPA1* (14) and *CHS* [R. L. Feinbaum and F. M. Ausubel, *Mol. Cell. Biol.* **8**, 1985 (1988)] probes have been described elsewhere.

49. Relative levels of transcripts were normalized to 18S ribosomal RNA levels (44) after PhosphorImager Storm 860 (Molecular Dynamics) quantification.
50. We thank Y. Kang for technical assistance; M. Ni for A22 seeds and original PIF3 clones; C. Fairchild for the phycocyanobilin; U. Hoecker for SPA1

cDNA; N. Wei for the *CHS* probe; E. Monte and M. Rodríguez-Concepción for support and discussion; all the lab members for discussion and support; and the *Arabidopsis* Biological Resource Center (Columbus, Ohio) for providing *hy5* (*hy5-1* allele) seeds. Supported by grants from the U.S. Department of Energy Basic Energy Sciences (DE-FG03-87ER13742) and U.S. Department of Agriculture Current Research Information Service (5335-21000-010-00D).

13 December 1999; accepted 25 February 2000

Template Boundary in a Yeast Telomerase Specified by RNA Structure

Yehuda Tzfati, Tracy B. Fulton, Jagoree Roy, Elizabeth H. Blackburn*

The telomerase ribonucleoprotein has a phylogenetically divergent RNA subunit, which contains a short template for telomeric DNA synthesis. To understand how telomerase RNA participates in mechanistic aspects of telomere synthesis, we studied a conserved secondary structure adjacent to the template. Disruption of this structure caused DNA synthesis to proceed beyond the normal template boundary, resulting in altered telomere sequences, telomere shortening, and cellular growth defects. Compensatory mutations restored normal telomerase function. Thus, the RNA structure, rather than its sequence, specifies the template boundary. This study reveals a specific function for an RNA structure in the enzymatic action of telomerase.

Telomerase, a ribonucleoprotein reverse transcriptase (RT), replenishes telomeric DNA that would otherwise be lost with each round of eukaryotic DNA replication (1). The telomerase complex contains an RNA subunit (TER), a catalytic RT protein (TERT), and several additional protein components (2). Telomerase is activated in most human cancers, and its ectopic expression can greatly extend the life-span of normal human cells in culture (3).

Telomerase RNAs are extremely divergent in sequence and vary in length from 146 nucleotides (nt) in the ciliate *Tetrahymena paravorax* (4) to 1544 nt in the budding yeast *Candida albicans* (5). Unlike other RTs, which perform extensive genome copying, telomerase copies only a small portion (termed the "template") of an intrinsic RNA moiety (6). This feature allows telomerase to synthesize onto telomeres a species-specific, 5- to 26-base-long repeated sequence (7). How telomerase specifies its template boundaries (where DNA synthesis initiates and where it ends on the TER sequence) is not understood.

Nontemplate regions have been previously shown to be required for telomerase activity (8, 9) and ribonucleoprotein (RNP) assembly (9,

10). To further investigate the participation of telomerase RNA in the enzymatic function of telomerase, we searched for conserved sequences and structural elements in budding yeast telomerase RNAs. We cloned and analyzed TER genes from four *Kluyveromyces* species closely related to *K. lactis* (11). The mature RNAs ranged in length from 930 nt in *K. aestuarii* to 1320 nt in *K. dozhanskii*. Sequence identity between any given pair of genes ranged from insignificant to about 70% overall identity. The computer program *mfold* (12) predicted extensive secondary structures for these RNA sequences, including a common feature shared by all five TERs: base pairing of the sequence immediately upstream of the template (pairing element B) (Fig. 1A) with a sequence 200 to 350 nt further upstream (pairing element A), located near the 5' end of the RNA. The region between the pairing elements (indicated by the dashed line in Fig. 1A and the dashed loop in Fig. 1B) was shown previously to be dispensable in *K. lactis* (9). The proximity of this conserved putative pairing region to the 5' end of the template led us to hypothesize that its function is to limit DNA synthesis, thereby defining the downstream boundary of the template.

To test this hypothesis, we constructed a series of mutations in the putative pairing region of the *K. lactis* TER gene (Fig. 1, C and D). We replaced the wild-type TER gene in *K. lactis* with the mutant genes by a vector-shuf-

Department of Microbiology and Immunology, University of California, San Francisco, San Francisco, CA 94143-0414, USA.

*To whom correspondence should be addressed. E-mail: telomer@itsa.ucsf.edu